Effective Properties of Carbon Nanotube and Piezoelectric Fiber Reinforced Hybrid Smart Composites

M. C. Ray

R. C. Batra

Department of Engineering Science and Mechanics,
Virginia Polytechnic Institute and State University,
MC 0219,
Blacksburg, VA 24061

We propose a new hybrid piezoelectric composite comprised of armchair single-walled carbon nanotubes and piezoelectric fibers as reinforcements embedded in a conventional polymer matrix. Effective piezoelectric and elastic properties of this composite have been determined by a micromechanical analysis. Values of the effective piezoelectric coefficient e_{31} of this composite that accounts for the in-plane actuation and of effective elastic properties are found to be significantly higher than those of the existing 1–3 piezoelectric composites without reinforced with carbon nanotubes. [DOI: 10.1115/1.3063633]

1 Introduction

The discovery of carbon nanotubes (CNTs) [1] has stimulated extensive research devoted to the prediction of their elastic properties through experiments and theoretical modeling. Treacy et al. [2] experimentally determined that CNTs have Young's modulus in the terapascal range. Li and Chou [3] linked structural and molecular mechanics (MM) approaches to compute elastic properties of CNTs. Sears and Batra [4] used three MM potentials to simulate axial and torsional deformations of a CNT assuming that the tube can be regarded as a hollow cylinder of mean diameter equal to that of the CNT. They found the wall thickness, Young's modulus, and Poisson's ratio of the CNT. Shen and Li [5] assumed that a CNT should be modeled as a transversely isotropic material with the axis of transverse isotropy coincident with the centroidal axis of the tube. They determined values of the five elastic constants by using a MM potential and an energy equivalence principle. Batra and Sears [6] proposed that the axis of transverse isotropy of a CNT is a radial line rather than the centroidal axis of the tube and found that Young's modulus in the radial direction equals about 1/4 of that in the axial direction. Batra and Gupta [7,8] determined the wall thickness and material moduli of a CNT based on the frequencies of axial, torsional, and radial breathing modes. Wu et al. [9] developed an atomistic based finite deformation shell theory for single-walled CNT and found its stiffness in tension, bending, and torsion. A great deal of research has also been carried out on the prediction of effective elastic properties of CNT-reinforced composites [10–12].

Piezoelectric composites, often called piezocomposites, have been used as distributed actuators and sensors. Piezocomposites (PZCs), usually comprised of an epoxy reinforced with a monolithic piezoelectric material (PZT), provide a wide range of effective material properties not offered by existing PZTs, are anisotropic, and are characterized by good conformability and strength. One of the commercially available PZCs is the lamina of vertically reinforced 1–3 PZCs [13] and is being effectively used as underwater and high frequency ultrasonic transducers, and in medical imaging devices. In a 1–3 PZC lamina the poling direction of PZT fibers is along the laminate thickness, and the top and the bottom surfaces of the lamina are electroded. Smith and Auld [14] used the micromechanical isostrain/isostress technique to determine the effective moduli of a PZC and found that the magnitude of the effective piezoelectric coefficient e_{33} is much larger than that of the effective piezoelectric coefficient e_{31}. Note that e_{33} determines the magnitude of the induced actuating stress along the fiber direction due to a unit electric field applied across the thickness of the PZC lamina while e_{31} gives the induced stress in the direction transverse to the fiber. Hence, the in-plane actuation of this PZC is negligible as compared with its out-of-plane actuation [15]. The control of bending deformations of a smart beam is generally attributed to the in-plane actuation induced by a PZT actuator. The in-plane actuation caused by the PZC can be enhanced by tailoring its effective piezoelectric coefficient e_{31}. Smith and Auld's [14] work also reveals that the magnitude of effective e_{31} can be increased by improving upon elastic properties of the matrix. Since CNT reinforcements noticeably strengthen the polymer matrix, the matrix can also be reinforced with CNT and PZT fibers to form a new hybrid PZC with improved effective piezoelectric coefficient e_{31}. Here, we find values of effective moduli of a hybrid PZC that we call nanotube reinforced hybrid piezoelectric composite (NRHPC) by using a micromechanics approach proposed by Smith and Auld [14], and Benveniste and Dvorak [16].

2 Effective Moduli of a NRHPC

Figure 1 shows a schematic sketch of a lamina of NRHPC with CNT and PZT fibers aligned vertically. The cross section of CNT and PZT fibers is shown as square for simplicity since it does not enter into calculations. The analysis applies to straight prismatic fibers with parallel centroidal axes and fibers perpendicular to the lamina. The CNT fibers are assumed to be transversely isotropic with the axis of transverse isotropy along the centroidal axis, and the PZT fibers are poled in the thickness direction. The representative volume element considered for the micromechanics analysis is comprised of a CNT fiber and a PZT fiber surrounded by a polymer matrix of the same volume fraction as that in the composite. Using rectangular Cartesian coordinate axes exhibited in Fig. 1, constitutive equations for the PZT, the CNT, and the polymer matrix material are

$$\{\sigma^p\} = [C^p]\{\varepsilon^p\} - \{e^p\}E_z, \quad \{\sigma^n\} = [C^n]\{\varepsilon^n\}, \quad \text{and} \quad \{\sigma^m\} = [C^m]\{\varepsilon^m\} \tag{1}$$

where

$$\{\sigma^r\} = [\sigma^r_x \quad \sigma^r_y \quad \sigma^r_z \quad \sigma^r_{yz} \quad \sigma^r_{xz} \quad \sigma^r_{xy}]^T,$$

$$\{\varepsilon^r\} = [\varepsilon^r_x \quad \varepsilon^r_y \quad \varepsilon^r_z \quad \varepsilon^r_{yz} \quad \varepsilon^r_{xz} \quad \varepsilon^r_{xy}]^T,$$

$$[C^r] = \begin{bmatrix} C^r_{11} & C^r_{12} & C^r_{13} & 0 & 0 & 0 \\ C^r_{12} & C^r_{22} & C^r_{23} & 0 & 0 & 0 \\ C^r_{13} & C^r_{23} & C^r_{33} & 0 & 0 & 0 \\ 0 & 0 & 0 & C^r_{44} & 0 & 0 \\ 0 & 0 & 0 & 0 & C^r_{55} & 0 \\ 0 & 0 & 0 & 0 & 0 & C^r_{66} \end{bmatrix},$$

Contributed by the Applied Mechanics Division of ASME for publication in the JOURNAL OF APPLIED MECHANICS. Manuscript received January 29, 2008; final manuscript received July 24, 2008; published online March 13, 2009 Review conducted by Yonggang Huang.

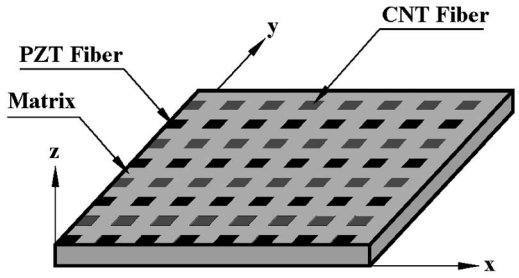

Fig. 1 Schematic sketch of a NRHPC comprised of a polymer matrix reinforced with CNT and PZT fibers

$$r = p,\ n,\ \text{and}\ m; \quad \{e^p\} = \begin{Bmatrix} e^p_{31} \\ e^p_{32} \\ e^p_{33} \\ 0 \\ 0 \\ 0 \end{Bmatrix} \tag{2}$$

In Eq. (1), superscripts p, n, and m denote, respectively, the PZT, the CNT, and the matrix. For the constituent phase r, σ^r_x, σ^r_y, and σ^r_z represent normal stresses in the x, y, and z, directions, respectively; ε^r_x, ε^r_y, and ε^r_z are the corresponding normal strains; σ^r_{xy}, σ^r_{yz}, and σ^r_{zx} are the shear stresses; ε^r_{xy}, ε^r_{yz}, and ε^r_{zx} are the shear strains; C^r_{ij} $(i, j = 1,2,3,\ldots,6)$ are elastic constants; and e^p_{31} and e^p_{33} are the piezoelectric coefficients of the PZT. A field variable and a material property without a superscript represent quantities for the hybrid composite. We assume that all fibers are perfectly bonded to the matrix, and hence satisfy the following isofield conditions [14,16]:

$$\begin{Bmatrix} \varepsilon^p_z \\ \sigma^p_x \\ \sigma^p_y \\ \sigma^p_{yz} \\ \sigma^p_{xz} \\ \sigma^p_{xy} \end{Bmatrix} = \begin{Bmatrix} \varepsilon^n_z \\ \sigma^n_x \\ \sigma^n_y \\ \sigma^n_{yz} \\ \sigma^n_{xz} \\ \sigma^n_{xy} \end{Bmatrix} = \begin{Bmatrix} \varepsilon^m_z \\ \sigma^m_x \\ \sigma^m_y \\ \sigma^m_{yz} \\ \sigma^m_{xz} \\ \sigma^m_{xy} \end{Bmatrix} = \begin{Bmatrix} \varepsilon_z \\ \sigma_x \\ \sigma_y \\ \sigma_{yz} \\ \sigma_{xz} \\ \sigma_{xy} \end{Bmatrix} \tag{3}$$

As a limitation of the above assumptions, Smith and Auld [14] mentioned that for applications as transducers, this homogenization technique yields good results when the fiber sizes and spacings are sufficiently small as compared with the acoustic wavelengths. Since diameters of CNTs are very small they can be closely packed to make spacing between any two of them much smaller than the acoustic wavelength. Also, the assumption of uniform axial strain in the thickness direction in the three phases is not strictly valid unless the top and the bottom faces are bonded to rigid membranes and are uniformly pressed in the axial direction. However, for CNTs and PZTs distributed uniformly with very little space between them, the assumption gives reasonable results for applications as actuators of beams and plates.

Following the procedure outlined in Ref. [14], the normal stress σ_z, the normal strains ε_x and ε_y, and the shear strains ε_{xz}, ε_{yz}, and ε_{xy} in the homogenized composite can be expressed in terms of the corresponding stresses and strains in the constituent phases. Thus using Eqs. (1) and (3), we obtain

$$\{\sigma\} = [C_1]\{\varepsilon^p\} + [C_2]\{\varepsilon^n\} + [C_3]\{\varepsilon^m\} - \{e_1\}E_z \tag{4}$$

$$\{\varepsilon\} = [V_1]\{\varepsilon^p\} + [V_2]\{\varepsilon^n\} + [V_3]\{\varepsilon^m\} \tag{5}$$

$$[C_4]\{\varepsilon^p\} - [C_5]\{\varepsilon^n\} = \{e_2\}E_z \tag{6}$$

$$[C_5]\{\varepsilon^n\} - [C_6]\{\varepsilon^m\} = 0 \tag{7}$$

in which

$$[C_1] = \begin{bmatrix} C^p_{11} & C^p_{12} & C^p_{13} & 0 & 0 & 0 \\ C^p_{12} & C^p_{22} & C^p_{23} & 0 & 0 & 0 \\ v_p C^p_{13} & v_p C^p_{23} & v_p C^p_{33} & 0 & 0 & 0 \\ 0 & 0 & 0 & C^p_{44} & 0 & 0 \\ 0 & 0 & 0 & 0 & C^p_{55} & 0 \\ 0 & 0 & 0 & 0 & 0 & C^p_{66} \end{bmatrix},$$

$$[C_2] = v_n \begin{bmatrix} 0 & 0 & 0 & 0 & 0 & 0 \\ 0 & 0 & 0 & 0 & 0 & 0 \\ C^n_{13} & C^n_{23} & C^n_{33} & 0 & 0 & 0 \\ 0 & 0 & 0 & 0 & 0 & 0 \\ 0 & 0 & 0 & 0 & 0 & 0 \\ 0 & 0 & 0 & 0 & 0 & 0 \end{bmatrix}$$

$$[C_3] = v_m \begin{bmatrix} 0 & 0 & 0 & 0 & 0 & 0 \\ 0 & 0 & 0 & 0 & 0 & 0 \\ C^m_{13} & C^m_{23} & C^m_{33} & 0 & 0 & 0 \\ 0 & 0 & 0 & 0 & 0 & 0 \\ 0 & 0 & 0 & 0 & 0 & 0 \\ 0 & 0 & 0 & 0 & 0 & 0 \end{bmatrix},$$

$$[C_4] = \begin{bmatrix} C^p_{11} & C^p_{12} & C^p_{13} & 0 & 0 & 0 \\ C^p_{12} & C^p_{22} & C^p_{23} & 0 & 0 & 0 \\ 0 & 0 & 1 & 0 & 0 & 0 \\ 0 & 0 & 0 & C^p_{44} & 0 & 0 \\ 0 & 0 & 0 & 0 & C^p_{55} & 0 \\ 0 & 0 & 0 & 0 & 0 & C^p_{66} \end{bmatrix}$$

$$[C_5] = \begin{bmatrix} C^n_{11} & C^n_{12} & C^n_{13} & 0 & 0 & 0 \\ C^n_{12} & C^n_{22} & C^n_{23} & 0 & 0 & 0 \\ 0 & 0 & 1 & 0 & 0 & 0 \\ 0 & 0 & 0 & C^n_{44} & 0 & 0 \\ 0 & 0 & 0 & 0 & C^n_{55} & 0 \\ 0 & 0 & 0 & 0 & 0 & C^n_{66} \end{bmatrix},$$

$$[C_6] = \begin{bmatrix} C^m_{11} & C^m_{12} & C^m_{13} & 0 & 0 & 0 \\ C^m_{12} & C^m_{22} & C^m_{23} & 0 & 0 & 0 \\ 0 & 0 & 1 & 0 & 0 & 0 \\ 0 & 0 & 0 & C^m_{44} & 0 & 0 \\ 0 & 0 & 0 & 0 & C^m_{55} & 0 \\ 0 & 0 & 0 & 0 & 0 & C^m_{66} \end{bmatrix}$$

$$[V_1] = \begin{bmatrix} v_p & 0 & 0 & 0 & 0 & 0 \\ 0 & v_p & 0 & 0 & 0 & 0 \\ 0 & 0 & 1 & 0 & 0 & 0 \\ 0 & 0 & 0 & v_p & 0 & 0 \\ 0 & 0 & 0 & 0 & v_p & 0 \\ 0 & 0 & 0 & 0 & 0 & v_p \end{bmatrix},$$

Table 1 Material properties of the constituent phases

Material	Source	C_{11} (GPa)	C_{12} (GPa)	C_{13} (GPa)	C_{33} (GPa)	C_{44} (GPa)	e_{31}^p (C/m^2)	e_{33}^p (C/m^2)
CNT (5,5)	[5]	668	404	184	2153	791	-	-
CNT (20,20)	[5]	148	144	43.5	545	227	-	-
CNT (50,50)	[5]	55.1	54.9	17.5	218	92	-	-
PZT5H	[14]	151	98	96	124	23	−5.1	27
Spurr	[14]	5.3	3.1	3.1	5.3	0.64	-	-

$$[V_2] = \begin{bmatrix} v_n & 0 & 0 & 0 & 0 & 0 \\ 0 & v_n & 0 & 0 & 0 & 0 \\ 0 & 0 & 0 & 0 & 0 & 0 \\ 0 & 0 & 0 & v_n & 0 & 0 \\ 0 & 0 & 0 & 0 & v_n & 0 \\ 0 & 0 & 0 & 0 & 0 & v_n \end{bmatrix}$$

$$[V_3] = \begin{bmatrix} v_m & 0 & 0 & 0 & 0 & 0 \\ 0 & v_m & 0 & 0 & 0 & 0 \\ 0 & 0 & 0 & 0 & 0 & 0 \\ 0 & 0 & 0 & v_m & 0 & 0 \\ 0 & 0 & 0 & 0 & v_m & 0 \\ 0 & 0 & 0 & 0 & 0 & v_m \end{bmatrix},$$

$$\{e_1\} = \begin{Bmatrix} e_{31}^p \\ e_{32}^p \\ v_p e_{33}^p \\ 0 \\ 0 \\ 0 \end{Bmatrix}, \quad \text{and} \quad \{e_2\} = \begin{Bmatrix} e_{31}^p \\ e_{32}^p \\ 0 \\ 0 \\ 0 \\ 0 \end{Bmatrix} \tag{8}$$

In Eq. (8) v_p, v_n, and v_m represent volume fractions of PZTs, CNTs, and the matrix, respectively. The elimination of field variables of the constituent phases from Eq. (4) to Eq. (7) yields the following constitutive relation for the proposed hybrid NRHPC:

$$\{\sigma\} = [C]\{\varepsilon\} - \{e\}E_z \tag{9}$$

where

$$[C] = [C_1][V_5]^{-1} + [C_7][V_6]^{-1}$$

$$\{e\} = \{e_1\} - [C_1][V_5]^{-1}[V_4][C_6]^{-1}\{e_2\} + [C_7][V_6]^{-1}[V_1][C_4]^{-1}\{e_2\}$$

$$[V_4] = [V_3] + [V_2][C_5]^{-1}[C_6], \quad [V_5] = [V_1] + [V_4][C_6]^{-1}[C_4]$$

$$[V_6] = [V_4] + [V_1][C_4]^{-1}[C_6] \quad \text{and} \quad [C_7] = [C_3] + [C_2][C_5]^{-1}[C_6] \tag{10}$$

Comparing Eq. (9) with the constitutive relation $(1)_1$ for a PZT, the effective piezoelectric coefficients e_{31}, e_{32}, and e_{33} of the NRHPC can be identified as $e_{31}=e(1)$, $e_{32}=e(2)$, and $e_{33}=e(3)$.

3 Results and Discussion

Material properties of CNTs, taken from Ref. [5], and of the PZT5H and the epoxy are listed in Table 1. Effective properties of the NRHPC, computed by simultaneously varying volume fractions of CNTs and PZT fibers, are compared with those given by Smith and Auld [14] for the PZT5H/epoxy composite.

Figure 2 depicts the variation of the effective piezoelectric coefficient e_{31} of the NRHPC with the PZT fiber volume fraction, and for different volume fractions of CNTs. It is clear from these plots that the value of e_{31} of the NRHPC is significantly enhanced by the addition of CNTs, and equals twice that of the 1–3 PZT5H/epoxy composites for $v_n=0.3$ and $v_p=0.4$. Furthermore, adding CNTs also improves values of elastic constants of the NRHPC over those of the existing 1–3 PZCs. As an example, we illustrate in Fig. 3 the variation of the effective elastic constant C_{33} with respect to the PZT5H fiber volume fraction for different volume fractions of CNTs. Using Eq. (10), values of other effective elastic and piezoelectric constants can be easily computed for any combination of volume fractions of CNTs and PZT fibers. Also, it is evident from Figs. 2 and 3 that for a particular value of v_p, values of the effective piezoelectric coefficient e_{31} and elastic properties increase with an increase in v_n. The significant improvement in

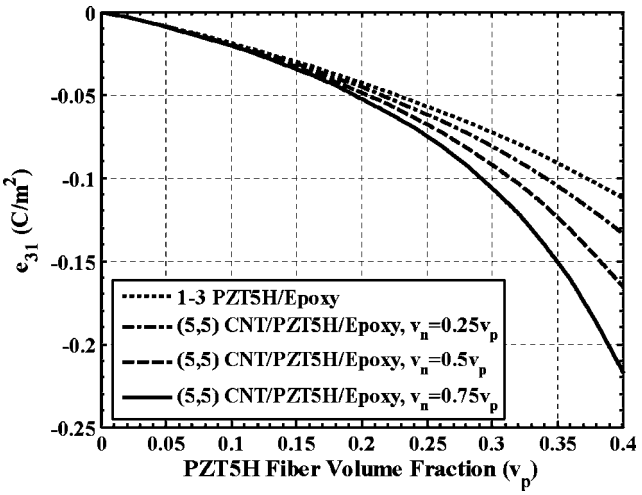

Fig. 2 Effective piezoelectric coefficient e_{31} of the NRHPC

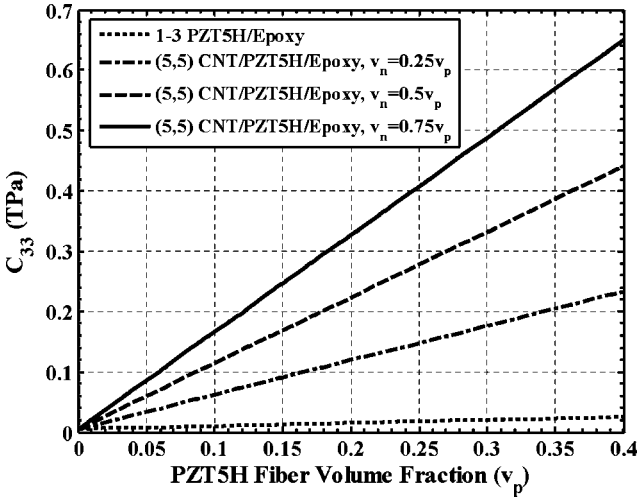

Fig. 3 Effective elastic coefficient C_{33} of the NRHPC

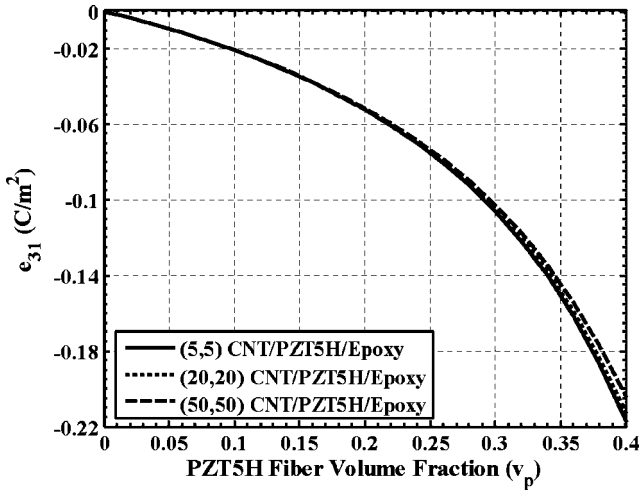

Fig. 4 For $v_n=0.75v_p$, variation of the effective piezoelectric coefficient e_{31} of the NRHPC with the diameter of CNTs

effective properties of the NRHPC is attributed to the fact that CNT reinforcements enhance the elastic properties of the matrix. It is also found that the value of the other in-plane effective piezoelectric coefficient e_{32} of the NRHPC equals that of the effective coefficient e_{31}. However, the addition of CNTs does not affect the value of the effective piezoelectric coefficient e_{33}. Results plotted in Figs. 4 and 5 reveal that as the diameter of the CNTs increases, magnitudes of both the e_{31} and the elastic moduli decrease because elastic moduli of a CNT decrease with an increase in the diameter of the CNT.

4 Conclusions

We have proposed a hybrid piezoelectric composite comprised of a polymer matrix and single-walled CNTs and piezoceramic (PZT5H) fibers aligned parallel to each other along the thickness of the laminate. The PZT5H fibers are poled in the thickness direction. Values of the effective piezoelectric coefficients e_{31} and e_{33} are proportional to the in-plane and the out-of-plane actuations, respectively, due to a voltage applied across the thickness of the hybrid lamina. Effective moduli of the hybrid lamina have been determined by using the isostrain and the isostress assumptions. It is found that the value of e_{31} of the proposed hybrid composite is significantly higher than that of the existing 1–3 piezocomposites [14] at the practically useful volume fraction of PZT fibers. For a fixed volume fraction of PZT fibers, the value of e_{31} for the hybrid composite increases with an increase in the volume fraction of CNTs, and that of e_{33} remains unaltered. Elastic moduli of the hybrid composite are also much larger than those of the existing 1–3 piezocomposites [15]. Because of increase in the value of e_{31}, the proposed hybrid composite can act as a distributed actuator for both in-plane and out-of-plane actuations while the in-plane actuation by the existing 1–3 piezocomposites is negligibly small [15].

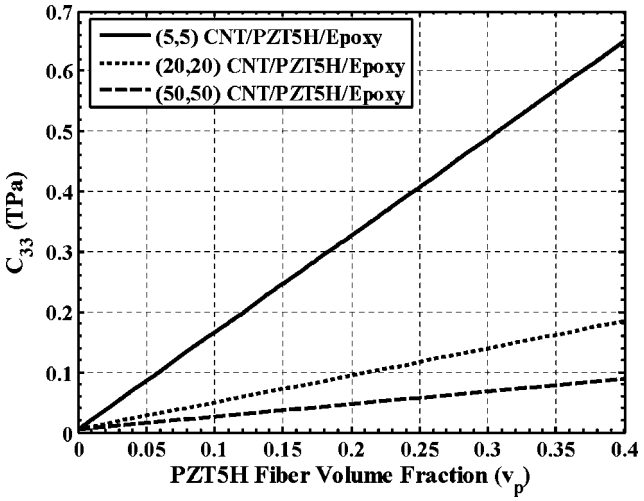

Fig. 5 For $v_n=0.75v_p$, variation of the effective elastic constant C_{33} of the NRHPC with the diameter of CNTs

Acknowledgment

This work was partially supported by the Office of Naval Research Grant No. N00014-98-06-0567 to Virginia Polytechnic Institute and State University with Dr. Y. D. S. Rajapakse as the program manager. Partial financial support from Virginia Tech's Institute of Critical Technologies and Sciences is gratefully acknowledged. Views expressed herein are those of authors, and neither of the funding agencies nor of VPI&SU.

References

[1] Iijima, S., 1991, "Helical Microtubes of Graphitic Carbon," Nature (London), **354**, pp. 56–58.
[2] Treacy, M. M. J., Ebbessen, T. W., and Gibson, J. M., 1996, "Exceptionally High Young's Modulus Observed for Individual Carbon Nanotubes," Nature (London), **381**, pp. 678–680.
[3] Li, C., and Chou, T. W., 2003, "A Structural Mechanics Approach for the Analysis of Carbon Nanotubes," Int. J. Solids Struct., **40**, pp. 2487–2499.
[4] Sears, A., and Batra, R. C., 2004, "Macroscopic Properties of Carbon Nanotubes From Molecular Mechanics Simulations," Phys. Rev. B, **69**, p. 235406.
[5] Shen, L., and Li, J., 2004, "Transversely Isotropic Elastic Properties of Single-Walled Carbon Nanotubes," Phys. Rev. B, **69**, p. 045415.
[6] Batra, R. C., and Sears, A., 2007, "Uniform Radial Expansion/Contraction of Carbon Nanotubes and Their Transverse Elastic Moduli," Modell. Simul. Mater. Sci. Eng., **15**, pp. 835–844.
[7] Gupta, S. S., and Batra, R. C., 2008, "Continuum Structures Equivalent in Normal Mode Vibrations to Single-Walled Carbon Nanotubes," Comput. Mater. Sci., **43**, pp. 715–723.
[8] Batra, R. C., and Gupta, S. S., 2008, "Wall Thickness and Radial Breathing Modes of Single-walled Carbon Nanotubes," ASME J. Appl. Mech., **75**, p. 061010.
[9] Wu, J., Hwang, K. C., and Huang, Y., 2008, "An Atomistic-Based Finite-Deformation Shell Theory for Single-Wall Carbon Nanotubes," J. Mech. Phys. Solids, **56**, pp. 279–292.
[10] Thostenson, E. T., and Chou, T. W., 2003, "On the Elastic Properties of Carbon Nanotube Based Composites: Modeling and Characterization," J. Phys. D, **36**, pp. 573–582.
[11] Odegard, G. M., Gates, T. S., Wise, K. E., Park, C., and Siochi, E. J., 2003, "Constitutive Modeling of Nanotube-Reinforced Polymer Composites," Compos. Sci. Technol., **63**, pp. 1671–1687.
[12] Song, Y. S., and Youn, J. R., 2006, "Modeling of Effective Elastic Properties for Polymer Based Carbon Nanotube Composites," Polymer, **47**, pp. 1741–1748.
[13] Piezocomposites, Materials System Inc., 543 Great Road, Littleton, MA 01560.
[14] Smith, W. A., and Auld, B. A., 1991, "Modeling 1-3 Composite Piezoelectrics: Thickness Mode Oscillations," IEEE Trans. Ultrason. Ferroelectr. Freq. Control, **38**(1), pp. 40–47.
[15] Ray, M. C., and Pradhan, A. K., 2007, "On the Use of Vertically Reinforced 1-3 Piezoelectric Composites for Hybrid Damping of Laminated Composite Plates," Mechanics of Advanced Materials and Structures, **14**, pp. 245–261.
[16] Benveniste, Y., and Dvorak, G. J., 1992, "Uniform Fields and Universal Relations in Piezoelectric Composites," J. Mech. Phys. Solids, **40**, pp. 1295–1412.